Lee *et al. Journal of NeuroEngineering and Rehabilitation* (2025) 22:89
https://doi.org/10.1186/s12984-025-01624-w

Journal of NeuroEngineering and Rehabilitation

RESEARCH **Open Access**

A wearable ankle-assisted robot for improving gait function and pattern in stroke patients

Su-Hyun Lee[1], Jinuk Kim[1,2], Hwang-Jae Lee[3*†] and Yun-Hee Kim[1,4*†]

Abstract

Background Hemiplegic gait after a stroke can result in a decreased gait speed and asymmetrical gait pattern. Normal gait patterns and speed are typically the ultimate goals of gait function in stroke rehabilitation. The purpose of this study was to investigate the immediate effects of the Gait Enhancing and Motivating System-Ankle (GEMS-A) on gait function and pattern in stroke patients with hemiplegia.

Methods A total of 45 eligible participants was recruited for the study. The experimental protocol consisted of overground gait at a comfortable speed under 2 conditions: free gait (FG) without robot assistance and robot-assisted gait (RAG). All measurement data were collected using a 3D motion capture system with 8 infrared cameras and 2 force plates.

Results Patients in the RAG condition had significantly increased gait speed, cadence, gait symmetry, and peak flexion angle and moment of the paretic ankle joint compared to the FG condition. Moreover, the RAG resulted in higher propulsive forces by altering peak ankle force generation compared with the FG.

Conclusion The findings of this study provide evidence that a newly developed wearable ankle-assist robot, the GEMS-A, is a potentially useful walking assist device for improving gait function and pattern in stroke patients with hemiplegia.

Trial registration NCT03767205 (first registration date: 02/12/2018, URL: https://register.clinicaltrials.gov).

Keywords Stroke, Gait, Ankle, Exoskeleton, Gait symmetry, Robotics

Background

Stroke occurs when the blood supply to part of the brain is either disrupted or reduced, possibly causing neurological impairments or deficits, including hemiparesis, cognitive and memory deficits, emotional disturbances, and communication difficulties [1, 2]. Hemiparesis following stroke results in unilateral primary impairment of the paretic leg, causing a disrupted walking pattern. Walking dysfunction is a common and relevant symptom for many who have experienced a stroke and causes difficulties in performing activities of daily living (ADL) [3]. Although most stroke patients eventually regain independent gait, many are not able to perform all ADL [4, 5], in part because of deficits in the voluntary motor control

†Hwang-Jae Lee and Yun-Hee Kim contributed equally to this work.

*Correspondence:
Hwang-Jae Lee
hwangjae.lee@samsung.com
Yun-Hee Kim
yunkim@skku.edu; yun1225.kim@gmail.com
[1]Department of Physical and Rehabilitation Medicine, Sungkyunkwan University School of Medicine, Suwon 16419, Republic of Korea
[2]Center for Neuroscience Imaging Research, Institute for Basic Science, Suwon 16419, Republic of Korea
[3]Bot Fit T/F, New Biz Team, Samsung Electronics, Suwon 16677, Republic of Korea
[4]Myongii Choonhey Rehabilitation Hospital, Seoul 07378, Republic of Korea

of the affected lower extremity [6]. Therefore, restoration of gait is the ultimate goal in rehabilitation programs for stroke patients [7]. A post-stroke hemiplegic gait pattern is characterized by asymmetry of spatiotemporal, kinematic, and kinetic parameters and muscle activity compared to healthy people [8]. Further, stroke survivors usually have a decreased stance phase, prolonged swing phase, and shorter single-limb support time of the paretic side and shorter stride length [9, 10]. These asymmetrical and inefficient walking patterns have been linked to reduced walking speed, increased risk of falls, and greater energy consumption [11–15].

Stroke generally damages the descending motor pathways of the central nervous system. Disrupted descending neural pathways to the paretic ankle joint cause poor voluntary control of the flexor muscles, spasticity of the extensor muscle, and a synergistic extension motor pattern [15], often accompanied with foot drop. Two major complications of foot drop are dropping and dragging of the forefoot on the ground during the swing phase and a forefoot or flat-foot initial contact in the stance phase [16]. Decreased activation of the anterior tibialis muscle and stiffness and/or contracture of the calf muscle cause reduced ankle dorsiflexion during the initial contact and mid-swing phases. Further, weakness of plantar flexor muscles mainly reduces stability and push-off power for forward propulsion [17]. To maintain sufficient foot clearance during walking, those with foot drop usually compensate either by hip hiking with exaggerated hip and knee flexion or hip circumduction with the body leaning on the unaffected side [18].

The human ankle joint plays an important role in shock absorption, propulsion, and balance while walking [19]. Post-stroke ankle impairment often requires the use of an ankle foot-orthosis (AFO), a solid plastic brace applied externally to the ankle-foot joint to provide foot clearance during the swing phase and medial or lateral stability during the stance phase. Although AFOs are the most popular daily-wear device due to their light weight, simplicity of use [20], compactness, and simplicity of design, they inhibit normal push-off during walking and reduce gait adaptability [21, 22]. In recent years, an active assist type of robotic device has been developed as an alternative to the passive ankle support provided by an AFO. In clinical practice, the ankle-assisted robotic device demonstrates that active power assistance at the ankle joint can facilitate gait restoration of patients presenting foot drop [23–26] and improve walking efficiency by providing physical movement assistance to help compensate for the asymmetric gait [27, 28].

Wearable exoskeletal robotics are promising novel technology to either restore or preserve mobility in individuals with motor disorders caused by stroke or spinal cord injury. Considering the importance of gait, research into robot-assisted therapy to improve gait function has been increasing rapidly, and the number of rehabilitation robotics has increased dramatically [29]. Existing ankle rehabilitation robots could be classified into platform-based ankle rehabilitation robots (stationary robots) and wearable ankle rehabilitation robots. Based on structure, wearable ankle rehabilitation robots are mainly categorized into rigid powered ankle exoskeletons and soft powered ankle exoskeletons [30]. As rigid-type exoskeletons, the Anklebot designed by the Massachusetts Institute of Technology (MIT) has the potential to address both forward propulsion and swing clearance, as well as balance problems because it is actuated in both the sagittal and frontal planes [28, 29, 31]. The powered exoskeleton [32] and ankle rehabilitation robot [33] were designed by North Carolina State University and the Chinese University of Hong Kong, respectively, for robot-assisted gait training of stroke survivors. Soft robotics, which have little to no rigid material, is an emerging field of research [31, 32, 34]. A soft robotic exosuit [35] and bio-inspired soft wearable robotic device [33] have been proposed by Harvard University and Carnegie Mellon University, respectively. These devices are placed over the paretic limb to enhance ground clearance and forward propulsion, contributing to a more normal walking gait post-stroke.

The purpose of this study was to examine the immediate effects of walking with ankle-assisted robotics on gait performance in stroke patients with hemiplegia. Here, a powered ankle exoskeleton called the Gait Enhancing and Motivating System-Ankle (GEMS-A) developed by Samsung Research (Seoul, Republic of Korea) provided dorsiflexion torque for minimizing foot slap at initial contact, foot clearance in the swing phase, and plantarflexion torque for push-off assistance (Fig. 1A). We tested the hypothesis that a single session of walking with the GEMS-A would lead to immediate improvements in gait, including spatiotemporal gait parameters, kinematics, and kinetics.

Methods

Participants

A total of 45 stroke patients with hemiplegia was recruited for this study and the characteristics of these subjects are shown in Table 1. Suitable candidates were identified as stroke patients > 3 months after a unilateral stroke. Participants had to be able to stand and walk independently or under supervision (Functional Ambulation Categories, range 3 to 5) [36]. Based on a clinical assessment, we excluded individuals with a modified Ashworth scale score greater than 3 or any other medical problems (e.g., severe dizziness, visual field defects, fracture, or serious cognitive problems) that affect walking capacity. Also, we excluded stroke patients with a foot size of

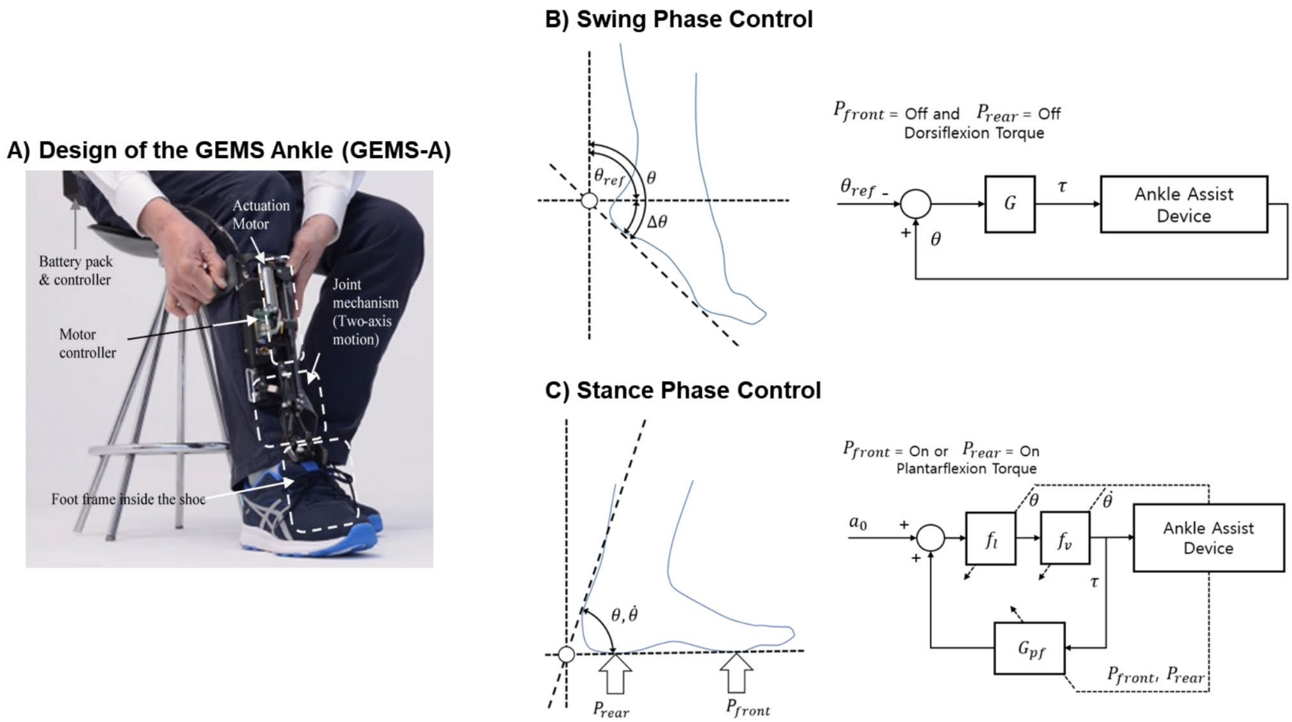

Fig. 1 (**A**) Configuration of the Gait Enhancing and Motivating System-Ankle (GEMS-A), (**B**) Ankle-assist control strategy during the swing phase with GEMS-A, and (**C**) Ankle-assist control strategy during the stance phase with GEMS-A

Table 1 Participant characteristics

Characteristics	Stroke subjects $n = 45$
Sex (male/female)	34/11
Age, years	54.1 (13.9)
Height, cm	167.9 (8.3)
Weight, kg	67.9 (11.3)
Stroke onset duration, y	2.8 (1.6)
Stroke type	
Ischemic/Hemorrhagic	25/20
Stroke location	
Cortical/Subcortical	13/32
Side of stroke	
Right/Left	26/19
FAC grade (3/4/5)	9/13/23

Values are presented as mean (standard deviation, SD)

FAC: functional ambulation category

230 mm or less or a stroke of 280 mm or more that are not suitable for GEMS-A. The experiment was conducted at Samsung Medical Center (Seoul, Republic of Korea), in accordance with institutional regulations and under the approval of the ethics committee of the Samsung Medical Center Institutional Review Board (Approval Number: SMC 2018-06-128). Written informed consent was obtained from all participants before inclusion in the study. The clinical trial registration of this study is NCT03767205 (first registration date: 02/12/2018, URL: https://register.clinicaltrials.gov).

The GEMS-A

The GEMS-A shown in Fig. 1A–C was designed to deliver assistive torque to the ankle joint for dorsi- and plantarflexion. The GEMS-A has a total weight of about 2.1 kg (device 1.4 kg and battery 0.7 kg) and can operate for more than 2 h. It consists of a ball-screw actuation mechanism that generates assistance power for the ankle joint, a joint mechanism that allows two-axis motions of the ankle joint, a foot frame that can be inserted into the shoe, and fastening belts that fit around the shank. The electrical components, including a battery and computing unit, are mounted in a waist pack. The ball-screw actuation mechanism includes a 74-watt DC motor, and its controller is mounted on the main body to generate assistance torque. The overall transmission ratio of the rotational angle of the motor to that of the ankle joint of the device is about 120, and a 1 mm ball-screw displacement corresponds to almost 1° of ankle joint rotation. The device can apply greater than 12 Nm of torque to the ankle joint. The joint mechanism allows two-axis ankle motions of active dorsi- and plantarflexion and passive inversion/eversion motions. This flexion provides assistance in pushing off from the ground, and the passive inversion/eversion permits the natural motion of the ankle when wearing the device. Two force sensors are attached to the toe and heel under the bottom of the foot frame to estimate the gait phase and measure forces between the foot frame and shoes. The users can adjust the height and lateral position of the rotation axis by changing the fastening position between the joint mechanism and the foot frame.

The GEMS-A is easy to use because it reacts like a normal ankle joint. To achieve this, the ankle assistance device uses a Hill-type muscle model [37] to operate similarly to the tibialis anterior and soleus muscles associated with the ankle. Human muscles have unique muscle length-force and contraction rate-force relationships that are modeled in the GEMS-A to mimic natural ankle reactions. Further, the planter flexure activation signal of the stance phase is generated by reflection-based positive feedback control and is not controlled by the central brain. In general, the control strategy of the GEMS-A aims to improve the walking performance of patients with small foot clearance and excessive asymmetric characteristics.

Control of the GEMS-A is divided into two steps: the swing step and the stance step. In the swing step, the foot is separated from the ground and moves forward to the center of the body, followed by heel landing. In this situation, both force-sensitive resistor (FSR) sensors are turned off, and the control routine of the stance phase is activated. To secure sufficient foot clearance, which is the distance between the ground and the foot, the device generates an additional plantar flexion torque at the swing phase, as shown in Fig. 1B. Back torque is applied through proportional control between plantar bending angles and criteria. This mimics a mechanism that prevents the foot from being pulled to the ground by the tibialis anterior muscle. This feature is useful for stroke patients whose ability to fold their ankles has been weakened due to rigidity or stiffness. During the stance phase, the foot is in contact with the ground to support the body and propel it forward. Patients with nerve or muscle problems cannot produce enough energy to push the body forward. To overcome these obstacles, the GEMS-A device supports push-off functions by providing the ankle joint a torque of up to 12 Nm. The stance stage begins when the front or rear FSR is activated. According to a previous study [36], the activation signal of the soleus muscle in the stance phase is generated by positive feedback in proportion to the power of the soleus itself. This activation signal stimulates the soleus muscle to exert a force determined by the joint angle θ and joint velocity $\dot{\theta}$. The programmed soleus muscle model of the GEMS-A generates a torque corresponding to the activation signal. The flowchart in Fig. 1C illustrates the flow of positive feedback in detail. Here, f_l is the relationship table between joint angle and torque, f_v is the relationship table of joint velocity and torque, and G_{pf} is positive feedback gain. Though the push-off function of the reflection algorithm is effective, when the positive feedback gain G_{pf} is fixed, torque is applied at inappropriate timing depending on the walking speed or individual walking characteristics, resulting in an uncomfortable fit. To obtain delicate control of the optimum timing of the push-off torque, the ratio between the pressures occurring at the front and rear FSRs was used as the positive feedback gain as in the equation below. This ratio allows us to infer the distance of the step through the center of pressure (COP) of the foot, enabling robust timing of the walking speed.

$$\mathrm{G_{pf}} \propto \frac{\mathrm{P_{front}}}{\mathrm{P_{rear}}}$$

Study design

All participants were acclimated to the GEMS-A through a single adaptation session of 30 min with a licensed physical therapist. Once the participants felt comfortable walking independently and the therapist was satisfied that the participants could walk safely, comfortably, and independently with the device, the participants walked at a self-selected speed along an 8-m walkway under two conditions in random order: (1) the FG condition without robot assistance, an 8-m walk without wearing the exoskeleton to measure baseline spatiotemporal, kinematic, and kinetic gait parameters and (2) the RAG condition: an 8-m walk while wearing the exoskeleton and using the assist torque. At least 10 min were required between the two conditions for wash-out.

Data collection and statistical analysis

The primary outcome measure was the change in self-selected gait speed between the two conditions. The secondary outcome measures were changes in spatiotemporal gait parameters and kinematic and kinetic data among the two conditions. The measures and procedures are described below.

Spatiotemporal gait parameters and kinematic data were measured using a 3-dimensional motion capture system with 8 infrared cameras (Motion Analysis Corporation, Santa Rosa, CA, USA), and kinetic data were obtained using 2 force plates (TF-4060-B, Tec Gihan, Kyoto, Japan) embedded midway along the walkway. Participants walked on a straight 8-meter walkway at their self-selected pace, without using any assistive devices or physical assistance, under two randomized conditions to collect data. The trajectories of the 19 markers placed on anatomical landmarks were recorded using the Helen Hayes marker set [38]. The motion capture system allowed us to identify each marker during collection, and marker position was recorded in real time. A standing calibration was used to obtain a rotation matrix for each limb segment and align the local (anatomical) reference frame for the thigh, shank, and foot to the global (laboratory) reference frame. Movement data were automatically converted to 3-dimensional coordinates with motion capture software, CORTEX version 64 6.2 (Motion Analysis Corporation, Santa Rosa, CA, USA). Subjects walked an average of 10 strides on the 8-meter walkway; an average of 5 strides per subject, excluding the acceleration and deceleration phases, was used in the analysis. Spatiotemporal, kinematic, and kinetic gait parameters were calculated for each gait cycle using Ortho Track 6.6.4 software (Motion Analysis Corporation, Santa Rosa, CA, USA).

Motion capture data were filtered using a Butterworth filter with a cutoff frequency of 6 Hz, applied as a 2-pass, 4th-order, zero-phase shift filter. Hip, knee, and ankle moments were initially calculated using inverse dynamics incorporating kinematics and ground reaction forces applied to the foot and the distance between the force application point and the segment's center of mass. Peak flexion angles of the hip and knee joints were calculated by averaging the maximum joint angles during each subject's gait cycle, while peak dorsiflexion and plantarflexion angles of the ankle joint were determined by averaging the maximum and minimum joint angles. Moment data were normalized by body weight, and the peak ankle plantarflexion moment measurements were averaged across trials for each subject. Vertical ground reaction force data were also normalized by body weight, and the values for the first peak, at the instant of loading response, and the second peak, during push-off (onset of forward propulsion), were averaged across trials for each subject. Cadence was measured in steps per minute, and stride length was defined as the distance between the initial contact of one foot and the subsequent initial contact of the same foot [39]. Spatiotemporal gait symmetry ratio (SR) was calculated using the following equations [40].

$$\text{Spatial step symmetry ratio (step length SR)} = \frac{\text{Paretic step length}}{\text{Nonparetic step length}} \tag{1}$$

$$\text{Stance symmetry ratio (stance SR)} = \frac{\text{Paretic stance time}}{\text{Nonparetic stance time}} \tag{2}$$

$$\text{Swing symmetry ratio (swing SR)} = \frac{\text{Paretic swing time}}{\text{Nonparetic swing time}} \tag{3}$$

The acquired data were analyzed using SPSS ver. 20 for Windows software (IBM Co., NY, USA) to assess changes in all gait performances related to RAG. All statistical analyses were performed with a significance level of $\alpha = 0.05$. To determine the appropriate statistical tests, we assessed the normal distribution of the data, based on which we applied parametric tests. The paired t test was used to compare all collected gait parameter data among the two conditions, and $p < 0.05$ was considered significant.

Table 2 Gait function as measured by Spatiotemporal gait parameters and gait symmetry ratio

	FG	RAG
Spatiotemporal gait parameters		
Gait speed, cm/s	50.78 (14.15)	60.86 (16.16)*
Cadence, step/min	77.9 (9.80)	84.57 (10.16)*
Stride length, cm	75.59 (13.18)	85.09 (15.75)*
Gait symmetry ratios		
Spatial step symmetry ratio	1.12 (0.22)	0.99 (0.18)*
Paretic step length, cm	44.08 (8.98)	43.12 (10.07)
Nonparetic step length, cm	40.67 (11.23)	44.12 (9.51)
Stance symmetry ratio	0.88 (0.08)	0.95 (0.09)*
Paretic stance time, % of stride	61.99 (5.83)	66.63 (4.71)
Nonparetic stance time, % of stride	70.93 (4.93)	70.42 (5.10)
Swing symmetry ratio	1.36 (0.24)	1.16 (0.28)*
Paretic swing time, % of stride	39.36 (6.45)	33.22 (4.40)
Nonparetic swing time, % of stride	29.41 (5.22)	29.58 (5.10)

Values are presented as mean (standard deviation, SD)

FG: free gait without robot assistance; RAG: robot-assisted gait

*Different from the FG condition ($p < 0.05$)

Results

The participant characteristics are summarized in Table 1. All participants completed testing under two experimental conditions, robot-assisted gait (RAG) and free gait (FG), without any major problems.

Spatiotemporal gait parameters

The specific values for spatiotemporal gait parameters and gait SR under the two conditions are given in Table 2. The gait speed in the RAG condition was significantly faster than in the FG condition ($p = 0.001$), and the cadence in the RAG condition was significantly higher than that in the FG condition ($p = 0.002$). The stride length in the RAG condition was also significantly longer than in the FG condition ($p < 0.001$). In addition, we observed statistically significant increases in spatial step SR, stance SR, and swing SR in the RAG condition compared to the FG condition ($p = 0.001$, $p = 0.001$, and $p = 0.003$, respectively).

Angles of the lower extremity joints

Figure 2 presents values for ankle, knee, and hip joint angles during gait and joint angle SR under the FG and RAG conditions. The peak flexion angles of the ankle, knee, and hip joints on the paretic side during the swing phase were significantly higher in the RAG condition compared to the FG condition ($p < 0.000$, $p = 0.049$, and

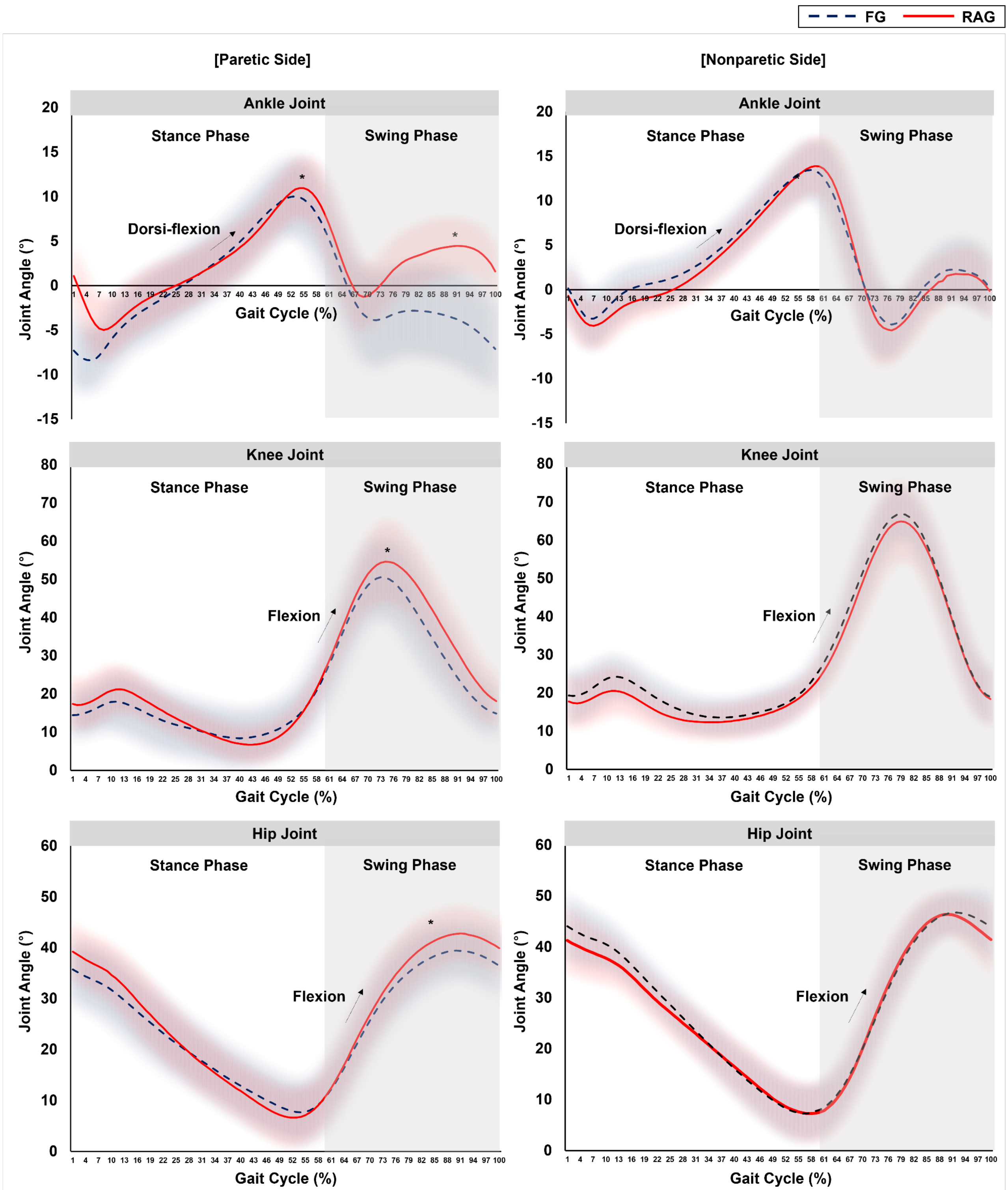

Fig. 2 (**A**) Comparison of the joint angles of paretic- and nonparetic sides during gait under the FG and RAG conditions. (**B**) Comparison of the joint angle symmetry ratio under the FG and RAG conditions (*$p < 0.05$). FG: free gait without robot assistance; RAG: robot-assisted gait

$p = 0.012$, respectively). Furthermore, the peak dorsiflexion angle of the ankle joint in the stance phase was higher in the RAG condition compared to the FG condition ($p < 0.000$). At initial contact, the foot on the paretic side had a more positive tilting angle from the ground in the RAG condition than in the FG condition.

Moment of the ankle joint

Figure 3 shows the ankle joint moment pattern (Nm/kg) during gait and ankle moment SR under the RAG and FG conditions. The peak moment of the ankle joint was significantly higher in the RAG condition than in the FG condition on both the paretic and nonparetic sides ($p = 0.035$ and $p = 0.042$, respectively). The peak moment of the ankle joint on the paretic side in the RAG condition increased by approximately 21% compared to the FG condition.

Vertical ground reaction force of the ankle joint

As illustrated in Fig. 4, an alteration in peak ankle power generation led to significantly higher first and second peaks of vertical ground reaction force (vGRF) on the paretic side in the RAG condition compared to the FG condition ($p = 0.042$ and $p = 0.048$, respectively). Under the RAG condition, peak vGRF on the paretic side was increased by about 17% (first peak, braking impulse) and 14% (second peak, propulsion impulse) compared to the FG condition.

Discussion

The aim of this study was to investigate the immediate effects of GEMS-A on gait performance in stroke patients with hemiplegia. The primary finding of this study was that spatiotemporal gait parameters including gait speed, cadence, stride length, and SR were improved significantly in the RAG condition compared to the FG condition. Furthermore, in gait pattern analysis, walking with GEMS-A significantly improved the motion of joint angles in the lower extremity of the paretic side. GEMS-A also had a positive effect on the joint moment and vGRF of the ankle joint on the paretic side. Therefore, the results of this study support our hypothesis that the GEMS-A had a positive effect on gait symmetry by improving not only the gait function but also the gait pattern on the paretic side.

Inadequate dorsiflexion control of the ankle joint on the paretic side after stroke was the primary determinant of gait speed and asymmetry. In addition, the limited ankle plantarflexion because of spasticity resulted in difficulty moving the center of gravity forward for the next step and led to shorter step length in the paretic leg compared with the nonparetic leg [41]. The shorter step length resulting from the ankle spasticity of the paretic side led to spatial asymmetry. Therefore, abnormal ankle movement after stroke was the most important factor in determining gait function and symmetry. Based on this ankle mechanism during gait, the results of our study demonstrated a clear increase in ankle dorsiflexion angle in stance (increase of 11.16%) and swing (increase of 27.8%) phases during gait in the RAG condition compared to the FG condition. On average, participants walked with 6.33 ± 1.05° greater peak ankle dorsiflexion on the paretic side during the swing phase in the RAG condition (4.42 ± 1.34°) compared to the FG condition (-1.91 ± 1.82°). This increase was seven times larger than the 0.90° minimal detectable change (MDC) score

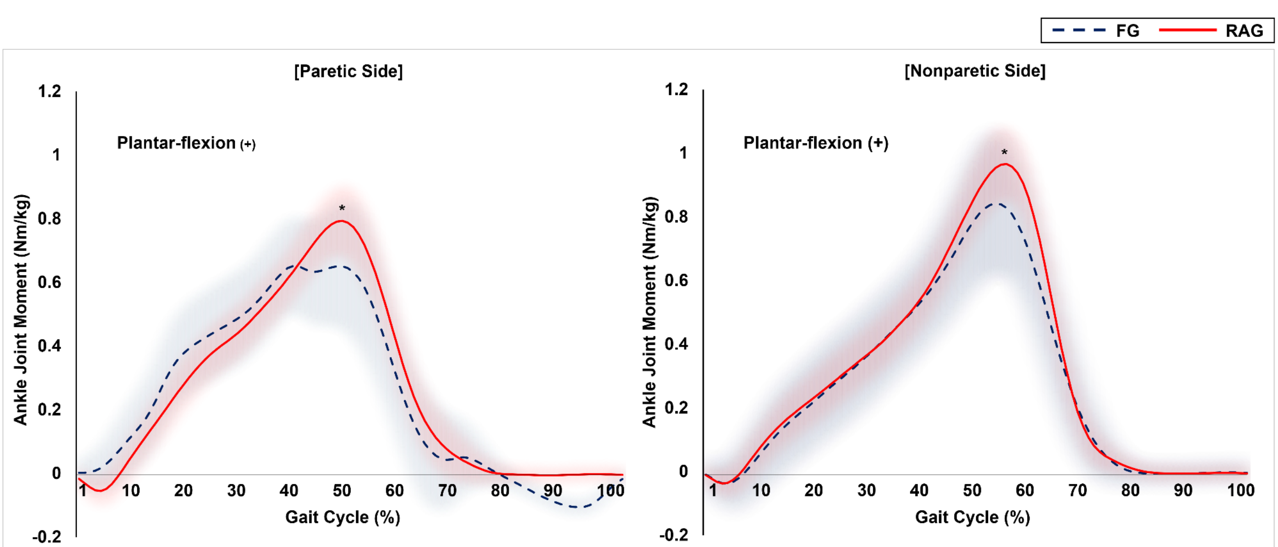

Fig. 3 (**A**) Comparison of the ankle moment of the paretic side during gait under the FG and RAG conditions. (**B**) Comparison of the ankle moment symmetry ratio under the FG and RAG conditions (*$p < 0.05$). FG: free gait without robot assistance; RAG: robot-assisted gait

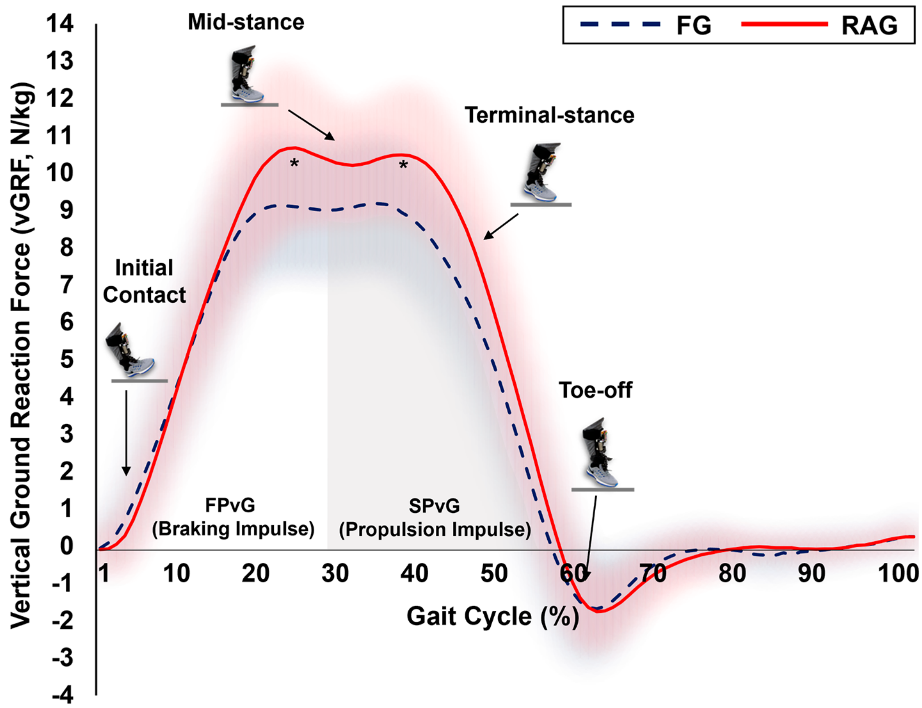

Fig. 4 Comparison of the vGRF (braking and propulsion impulse stages) of the paretic side during FG and RAG (*$p < 0.05$). vGRF: vertical ground reaction force, FG: free gait without robot assistance; RAG: robot-assisted gait, FPvG: first peak vertical ground reaction force, SPvG: second peak vertical ground reaction force

reported for this critical metric of swing phase gait function [42]. In studies examining the immediate effects of unpowered versus powered ankle rehabilitation robots [21, 22], the increase in peak dorsiflexion angle on the paretic side during the swing phase was less than 5°. In contrast, multiple training sessions contributed to a significant increase greater than 5° in the dorsiflexion angle on the paretic side [43, 44]. The results may be related to multiple sessions of walking with powered ankle exoskeletons. Our study demonstrated an immediate increase greater than 5°, indicating that gait training with GEMS-A may result in even greater improvements.

More interestingly, we also observed a significant increase in peak flexion angle of the hip and knee joints during the swing phase in the RAG condition (Fig. 2A). The increased ankle dorsiflexion movement may deliver flexor synergic movements to the knee and hip joints for a clear swing stage because the increase of vGRF in the propulsion impulse stage and ankle plantar flexion moment produces greater mechanical ankle flexion movement during the initial swing phase [45–47]. We demonstrated a clear increase in peak plantar flexion moment of ankle joint and vGRF on the paretic side in the RAG condition. This increased ankle movement and power could deliver higher flexion energy for forward progression of the paretic leg, which could be transmitted as flexion synergic energy to the hip and knee joint. Consequently, this wearable ankle-assist robot indirectly increased hip and knee flexion strategies during the swing phase, while directly enhancing ankle movement strategies during walking in stroke patients.

Another finding of this study was the significantly increased overall gait symmetry (for instance, spatial step, stance and swing time SRs) between the paretic- and nonparetic side when walking with the GEMS-A (Table 2). Gait speed has been recognized as the best indicator of gait function in stroke patients, and it has an increase in speed related to a perceived improvement in quality of life [47]. However, recent studies have suggested that the level of asymmetry in different gait parameters could be more relevant than walking speed in relation to the degree of paretic leg impairment and the compensatory mechanisms of gait [48]. According to previous research, impairment of ankle plantarflexion influenced the severity of spatial step asymmetry in stroke patients [49], and gait asymmetry and speed have been reported to be strongly correlated [50]. Moreover, both gait speed and asymmetry have shown a strong correlation with paretic lower limb muscle strength and movement, joint peak torque, spasticity, and dynamic balance [51]. Our study demonstrated a significant improvement in spatial step symmetry with increased ankle plantarflexion moment and vGRF in the RAG condition. The peak ankle plantarflexion moment on the paretic side in the RAG condition increased by approximately 21% compared to the FG condition. Notably, this increase is greater than the short-term 16% increase in the paretic plantarflexion moment during powered walking trials compared to an unassisted walking condition in a previous study [30]. Furthermore, we observed a significant increase in gait speed, with a 19.85% (10.08 cm/s) improvement in the RAG condition compared to the FG condition. This increase exceeds the minimal clinically important difference (MCID), which represents the smallest change in gait speed that is considered clinically meaningful for stroke patients [51]. Overall, our results suggest that a positive change in gait patterns was observed in the RAG condition, with improvements in joint angle, moment, and vGRF, as well as in gait functions such as speed and symmetry.

Over the past few decades, various ankle rehabilitation robots have been developed and have demonstrated significant potential in assisting or rehabilitating the ankle joints of stroke survivors, ultimately improving gait function. GEMS-A is a wearable powered ankle exoskeleton that actuates plantarflexion and dorsiflexion movements of the ankle joint and can be used for overground walking with programmable control. Although rigid-type exoskeletons have some disadvantages, such as being bulky and heavy, compared to the powered ankle exoskeletons, GEMS-A is a compact, lightweight (a total weight of about 2.1 kg), and portable device that can be used to assist impaired users in daily life activities. The actuator is a key factor for ankle rehabilitation robots and determines the assistance torque provided by the robot in gait training. Sufficient torque is essential for effective functional assistance to promote gait rehabilitation. MIT's Anklebot, which is powered by two linear actuators, has been used for gait rehabilitation post stroke. The design and function are similar to those of the GEMS-A, which allows two-axis ankle motions of active dorsi- and plantarflexion and passive inversion/eversion. However, MIT's Anklebot has some disadvantages such as being heavy (3.6 kg), bulky, and tethered. In comparison, a bio-inspired soft wearable robotic device proposed by Carnegie Mellon University is lightweight, provides multi-degree of freedom assistance, and does not limit natural degrees of freedom; however, the device is difficult to operate and not portable [17, 33]. A previous study demonstrated that adding a weight of 2.5 kg to the leg in a short period did not change the kinematics of the lower extremities [52]. Similarly, unilateral loading of 3.6 kg with MIT's Anklebot did not significantly alter the gait pattern of chronic stroke survivors [53]. Nevertheless, the heavy weight of the ankle rehabilitation robot would increase the burden on the lower limbs of stroke survivors, change the gait pattern, and adversely affect longtime gait training and rehabilitation. Therefore, lightweight and high-output-torque actuators need to be further developed.

The limitations of this study include that we only investigated the immediate effects of GEMS-A on gait function, pattern, and symmetry in stroke patients, and that the acclimatization session may have influenced the FG condition. Further studies are needed to confirm the effects of adaptation following familiarization with the GEMS-A, and to demonstrate the impact of gait training using the GEMS-A in stroke patients with hemiparesis. In addition, the study protocol was designed with consideration for patient fatigue, and the participants walked under two conditions: FG and RAG. Therefore, we could not investigate the impact of the robot's weight on gait patterns and parameters. Further research could consider the differences between normal gait and non-assisted conditions. Finally, the low statistical power of this study with a small number of subjects prevents generalization of the results to the entire stroke population. According to a previous study, normalizing the kinetics of gait may have benefits for various neurologically impaired patients. It has been postulated that the introduction of normal moment switching at a joint has a potential motor learning effect, and that permanent changes in gait may be possible. The possibility of such motor learning effects may lead to important opportunities in rehabilitation intervention [54]. Therefore, a gait training study using the GEMS-A with follow-up in a larger sample size will be conducted in the near future. Additionally, future research should include an evaluation of user satisfaction and usability of the robot as these factors are crucial for effective implementation of such devices in rehabilitation settings.

In conclusion, this study demonstrated the feasibility and potential immediate benefits of wearing a GEMS-A on hemiparetic gait. Improvements in the gait patterns of stroke patients using the GEMS-A were observed in the joint angle of the paretic lower extremity, ankle joint plantarflexion moment, and vGRF. Comprehensively, improvements in gait function with GEMS-A were observed in gait speed, cadence, and gait symmetry, with positive effects on overall gait pattern. The findings of this study provide evidence that a newly developed wearable ankle-assist robot, the GEMS-A, is a potentially useful walking assist device for improving gait pattern and function in stroke patients with hemiplegia.

Acknowledgements
The authors would like to thank all the participants who collaborated in this study.

Author contributions
YHK and HJL contributed to experimental design, experimental progress, data analysis and interpretation. HJL, SHL and JK contributed to setting up the experiment and collecting data. Also, SHL contributed to write a draft of

the manuscript. YHK gave conceptual advice and edited the manuscript. All authors reviewed the manuscript.

Funding
This study was supported by Samsung Electronics (PHO0180291) and by the Korea Medical Device Development Fund grant funded by the Korean government (Ministry of Science and ICT, Ministry of Trade, Industry and Energy, Ministry of Health & Welfare, and Ministry of Food and Drug Safety) (KMDF-RS-2022–00140478).

Data availability
No datasets were generated or analysed during the current study.

Declarations

Ethics approval and consent to participate
The study was approved by the ethics committee of the Samsung Medical Center Institutional Review Board (approval number: SMC 2018-06-128).

Consent for publication
Consent to publish was obtained from all the participants.

Competing interests
The authors declare no competing interests.

Received: 14 June 2024 / Accepted: 7 April 2025
Published online: 22 April 2025

References

1. Belda-Lois J-M, et al. Rehabilitation of gait after stroke: a review towards a top-down approach. J Neuroeng Rehabil. 2011;8:1–20.
2. das Nair R, et al. Cognitive rehabilitation for memory deficits after stroke. Cochrane Database Syst Reviews. 2016(9).
3. Beyaert C, Vasa R, Frykberg GE. Gait post-stroke: pathophysiology and rehabilitation strategies. Neurophysiologie Clinique/Clinical Neurophysiol. 2015;45(4–5):335–55.
4. Flansbjer U-B, et al. Reliability of gait performance tests in men and women with hemiparesis after stroke. J Rehabil Med. 2005;37(2):75–82.
5. Sánchez N, et al. Lower extremity motor impairments in ambulatory chronic hemiparetic stroke: evidence for lower extremity weakness and abnormal muscle and joint torque coupling patterns. Neurorehabilit Neural Repair. 2017;31(9):814–26.
6. Taveggia G, et al. Conflicting results of robot-assisted versus usual gait training during postacute rehabilitation of stroke patients: a randomized clinical trial. Int J Rehabil Res. 2016;39(1):29–35.
7. Szopa A, et al. The link between weight shift asymmetry and gait disturbances in chronic hemiparetic stroke patients. Clin Interv Aging. 2017;1(12):2055–62.
8. Li S, Francisco GE, Zhou P. Post-stroke hemiplegic gait: new perspective and insights. Front Physiol. 2018;9:1021.
9. Patterson KK, et al. Gait asymmetry in community-ambulating stroke survivors. Arch Phys Med Rehabil. 2008;89(2):304–10.
10. Weerdesteijn V, et al. Falls in individuals with stroke. 2008.
11. Harris JE, et al. Relationship of balance and mobility to fall incidence in people with chronic stroke. Phys Ther. 2005;85(2):150–8.
12. Kramer S, et al. Energy expenditure and cost during walking after stroke: a systematic review. Arch Phys Med Rehabil. 2016;97(4):619–32. e1.
13. Wei T-S, et al. Gait asymmetry, ankle spasticity, and depression as independent predictors of falls in ambulatory stroke patients. PLoS ONE. 2017;12(5):e0177136.
14. Awad LN, et al. Walking speed and step length asymmetry modify the energy cost of walking after stroke. Neurorehabilit Neural Repair. 2015;29(5):416–23.
15. KEMU MA. Kinetics and kinematics of loading response in stroke patients (a review article). Annals King Edw Med Univ. 2008;14(4):143–143.
16. Yeung L-F, et al. Randomized controlled trial of robot-assisted gait training with dorsiflexion assistance on chronic stroke patients wearing ankle-foot-orthosis. J Neuroeng Rehabil. 2018;15:1–12.
17. Shi B, et al. Wearable ankle robots in post-stroke rehabilitation of gait: a systematic review. Front Neurorobotics. 2019;13:63.
18. Alam M, Choudhury IA, Mamat AB. Mechanism and design analysis of articulated ankle foot orthoses for Drop-Foot. Sci World J. 2014;2014(1):867869.
19. Vistamehr A, Kautz SA, Neptune RR. The influence of solid ankle-foot-orthoses on forward propulsion and dynamic balance in healthy adults during walking. Clin Biomech Elsevier Ltd. 2014;29(5):583–9.
20. Van Swigchem R, et al. The capacity to restore steady gait after a step modification is reduced in people with poststroke foot drop using an ankle-foot orthosis. Phys Ther. 2014;94(5):654–63.
21. Awad LN, et al. A soft robotic exosuit improves walking in patients after stroke. Sci Transl Med. 2017;9(400):eaai9084.
22. Blanchette AK, et al. Modifications in ankle dorsiflexor activation by applying a torque perturbation during walking in persons post-stroke: a case series. J Neuroeng Rehabil. 2014;11:1–11.
23. Bae J, et al. A lightweight and efficient portable soft exosuit for paretic ankle assistance in walking after stroke. In: 2018 IEEE International Conference on Robotics and Automation (ICRA); 2018. IEEE.
24. Martini E, et al. Gait training using a robotic hip exoskeleton improves metabolic gait efficiency in the elderly. Sci Rep. 2019;9(1):7157.
25. Lee H-J, et al. A wearable hip assist robot can improve gait function and cardiopulmonary metabolic efficiency in elderly adults. IEEE Trans Neural Syst Rehabil Eng. 2017;25(9):1549–57.
26. Chang WH, Kim Y-H. Robot-assisted therapy in stroke rehabilitation. J Stroke. 2013;15(3):174.
27. Krebs HI, et al. Pediatric anklebot: pilot clinical trial. In: 2016 6th IEEE International Conference on Biomedical Robotics and Biomechatronics (BioRob); 2016. IEEE.
28. Roy A, et al. Anklebot-assisted locomotor training after stroke: A novel deficit-adjusted control approach. In: 2013 IEEE International Conference on Robotics and Automation; 2013. IEEE.
29. Blaya JA, Herr H. Adaptive control of a variable-impedance ankle-foot orthosis to assist drop-foot gait. IEEE Trans Neural Syst Rehabil Eng. 2004;12(1):24–31.
30. Takahashi KZ, Lewek MD, Sawicki GS. A neuromechanics-based powered ankle exoskeleton to assist walking post-stroke: a feasibility study. J Neuroeng Rehabil. 2015;12:1–13.
31. Kwon J, et al. A soft wearable robotic ankle-foot-orthosis for post-stroke patients. IEEE Rob Autom Lett. 2019;4(3):2547–52.
32. Majidi C. Soft robotics: a perspective—current trends and prospects for the future. Soft Rob. 2014;1(1):5–11.
33. Park Y-L, et al. Design and control of a bio-inspired soft wearable robotic device for ankle–foot rehabilitation. Bioinspir Biomim. 2014;9(1):016007.
34. Mehrholz J, et al. Predictive validity and responsiveness of the functional ambulation category in hemiparetic patients after stroke. Arch Phys Med Rehabil. 2007;88(10):1314–9.
35. Winters JM. *Hill-based muscle models: a systems engineering perspective*, in *Multiple muscle systems: biomechanics and movement organization*. Springer; 1990. pp. 69–93.
36. Geyer H, Herr H. A muscle-reflex model that encodes principles of legged mechanics produces human walking dynamics and muscle activities. IEEE Trans Neural Syst Rehabil Eng. 2010;18(3):263–73.
37. Collins TD, et al. A six degrees-of-freedom marker set for gait analysis: repeatability and comparison with a modified Helen Hayes set. Gait Posture. 2009;30(2):173–80.
38. Guzik A, et al. Relationships between walking velocity and distance and the symmetry of temporospatial parameters in chronic post-stroke subjects. Acta Bioeng Biomech. 2017;19(3).
39. Ardestani MM, et al. From normal to fast walking: impact of Cadence and Stride length on lower extremity joint moments. Gait Posture. 2016;46:118–25.
40. Lee H-J, et al. Training for walking efficiency with a wearable hip-assist robot in patients with stroke: a pilot randomized controlled trial. Stroke. 2019;50(12):3545–52.
41. Kim CM, Eng JJ. Symmetry in vertical ground reaction force is accompanied by symmetry in Temporal but not distance variables of gait in persons with stroke. Gait Posture. 2003;18(1):23–8.
42. Kesar TM, et al. Minimal detectable change for gait variables collected during treadmill walking in individuals post-stroke. Gait Posture. 2011;33(2):314–7.
43. Roy A, et al. Facilitating push-off propulsion: A biomechanical model of ankle robotics assistance for plantarflexion gait training in stroke. In: 5th IEEE RAS/EMBS International Conference on Biomedical Robotics and Biomechatronics; 2014. IEEE.

44. Forrester LW, et al. Task-specific ankle robotics gait training after stroke: a randomized pilot study. J Neuroeng Rehabil. 2016;13:1–6.
45. Winter DA. Kinematic and kinetic patterns in human gait: variability and compensating effects. Hum Mov Sci. 1984;3(1–2):51–76.
46. Siegel KL, Kepple TM, Stanhope SJ. Joint moment control of mechanical energy flow during normal gait. Gait Posture. 2004;19(1):69–75.
47. Polese JC, et al. The effects of walking sticks on gait kinematics and kinetics with chronic stroke survivors. Clin Biomech Elsevier Ltd. 2012;27(2):131–7.
48. Allen JL, Kautz SA, Neptune RR. Step length asymmetry is representative of compensatory mechanisms used in post-stroke hemiparetic walking. Gait Posture. 2011;33(4):538–43.
49. Lin P-Y, et al. The relation between ankle impairments and gait velocity and symmetry in people with stroke. Arch Phys Med Rehabil. 2006;87(4):562–8.
50. Hsu A-L, Tang P-F, Jan M-H. Analysis of impairments influencing gait velocity and asymmetry of hemiplegic patients after mild to moderate stroke. Arch Phys Med Rehabil. 2003;84(8):1185–93.
51. Perera S, et al. Meaningful change and responsiveness in common physical performance measures in older adults. J Am Geriatr Soc. 2006;54(5):743–9.
52. Rossi S, et al. Feasibility study of a wearable exoskeleton for children: is the gait altered by adding masses on lower limbs? PLoS ONE. 2013;8(9):e73139.
53. Khanna I, et al. Effects of unilateral robotic limb loading on gait characteristics in subjects with chronic stroke. J Neuroeng Rehabil. 2010;7:1–8.
54. Butler P, Farmer S, Major R. Improvement in gait parameters following late intervention in traumatic brain injury: a long-term follow-up report of a single case. Clin Rehabil. 1997;11(3):220–6.

Publisher's note